


# Exploring the interior of cuticles and compressions of fossil plants by FIB-SEM milling and image microscopy

L. M. SENDER , I. ESCAPA, A. BENEDETTI, R. CÚNEO & J. B. DIEZ

Área de Paleontología, Facultad de Ciencias, Edificio C (Geológicas), Universidad de Zaragoza (Zaragoza), C/ Pedro Cerbuna s/n, Spain

**Key words.** FIB, fossil plant compressions, fossil plant cuticle, microstructures, SEM, ultrastructures.

## Summary

We present the first study of cuticles and compressions of fossil leaves by Focused Ion Beam Scanning Electron Microscopy (FIB-SEM). Cavities preserved inside fossil leaf compressions corresponding to substomatal chambers have been observed for the first time and several new features were identified in the cross-section cuts. These results open a new way in the investigation of the three-dimensional structures of both micro- and nanostructural features of fossil plants. Moreover, the application of the FIB-SEM technique to both fossils and extant plant remains represent a new source of taxonomical, palaeoenvironmental and palaeoclimatic information.

## Introduction

FIB-SEM instruments were initially developed for the study of *in situ* nanostructures in industrial materials (Orloff *et al.*, 2003). They eventually found applications in a great variety of research areas, such as lithography and nanodevice developments (Fujii & Kaito, 2005; Moberly *et al.*, 2007; Volkert & Minor, 2007; Santschi *et al.*, 2009; Javed *et al.*, 2014), petrology and mineralogy (Heaney *et al.*, 2001; Lee *et al.*, 2003; Wirth, 2004; de Winter *et al.*, 2009; Stokes & Hayles, 2009), biological materials (Drobne *et al.*, 2005; Nalla *et al.*, 2005; Orso, 2005; Milani *et al.*, 2007; Moberly *et al.*, 2007; de Winter *et al.*, 2009; Marko, 2010; Grandfield & Engqvist, 2012; Rigort *et al.*, 2012; Hoffmann *et al.*, 2015; Wagenknecht *et al.*, 2015), extant pollen grains and plant tissues (House & Balkwill, 2013; Bhawana *et al.*, 2014), and the analysis of forensic data (Milani *et al.*, 2012).

This microscopy technique has a great potential in different fields of palaeontology, including taxonomic studies and palaeoecological inferences (Schiffbauer & Xiao, 2011; Cunningham *et al.*, 2014). However, despite its extremely high

spatial resolution it has received very little attention, and has only been applied to acritarchs and other Precambrian microfossils (Kempe *et al.*, 2005; Schiffbauer & Xiao, 2009; Wacey *et al.*, 2012; Pang *et al.*, 2013), bones of sauropod dinosaurs (Dumont *et al.*, 2011) and fossilised bird feathers (Vitek *et al.*, 2013). Its use in palaeobotanical studies is even more rare, having been limited to imaging the internal layered disposition of Triassic spores embedded in metamorphic rocks (Bernard *et al.*, 2007) or the organisation of Early Cretaceous spore masses and structure of pollen grains (Villanueva-Amadoz *et al.*, 2012, 2014). In this sense, its application to fossil cuticles and compressions could be particularly promising because it allows the analysis of ultrastructural organisation of fossil leaves and microstructures.

The cuticle in vegetal species (according to Kerp, 1990) is a 'thin extracellular layer that overlies the epidermis and protects the plant against drought and moisture stress'. The cuticle has a highly resistant chemical composition with regard to degradation and is a perfect 'copying machine' of the plant epidermis, thus it is of major importance in the study of fossil plants, in particular leaves and fruits (Spicer & Thomas, 1986). Since the advent of the modern cuticular analysis on fossils in the 1930s by Thomas Harris, microscopic techniques applied to the study of the outermost plant layer have been continuously improved (Florin, 1933; Alvin, 1970; Archangel-sky *et al.*, 1986; Kerp, 1990; Guignard *et al.*, 1998, 2004; Krings, 2000; Zodrow *et al.*, 2010). Particularly significant are the improvements in light microscopy, due to the evolution of light and scanning electron microscopy (SEM; e.g. Alvin, 1970), fluorescence microscopy (e.g. Van Gijzel, 1977) and Transmission Electron Microscopy (TEM; e.g. Archangel-sky *et al.*, 1986). More recently, synchrotron X-ray analysis was included (e.g. Cunningham *et al.*, 2014) to achieve a more complete view of cuticular features. Each technique has been able to add more information in terms of mega, micro and ultrastructure of the fossil cuticles, and they have collectively provided an improved understanding of features and structures contained within this plant layer. The use of cuticle information is relevant in the study of fossil plants from a

Corresponding to: L. M. Sender, Área de Paleontología, Facultad de Ciencias, Edificio C (Geológicas), Universidad de Zaragoza (Zaragoza), C/ Pedro Cerbuna s/n. 50009 Zaragoza, SPAIN. Tel: +34 619915838; fax: +34 976761106; e-mail: lmsender@yahoo.es

taxonomic (Harris, 1979; Stockey, 1994; Taylor *et al.*, 2009; Sreelakshmi *et al.*, 2014; Tosolini *et al.*, 2015 and references therein), palaeochemical (Mösle *et al.*, 1998; Nguyen-Tu *et al.*, 1999; Zodrow *et al.*, 2010 and references therein) and palaeoenvironmental perspective (McElwain & Chaloner, 1996; Haworth *et al.*, 2005; Haworth & McElwain, 2008 and references therein). The latter application has been widely investigated as of recent, due to the possibility of establishing past atmospheric composition and inferring palaeotemperatures related to the proportions between different gases (CO<sub>2</sub> and O<sub>2</sub>) present in the palaeoatmospheres (e.g. McElwain & Chaloner 1995; McElwain, 1998; Royer, 2001, 2008; Haworth *et al.*, 2011; Steinthorsdottir *et al.*, 2011; Steinthorsdottir & Vajda, 2015).

Despite the improvements mentioned above, observing the ultrastructure of fossil cuticles, especially when manual preparation is required, can be tedious and time consuming. In this contribution we use a powerful new ultrastructural observation technique, FIB-SEM, to characterise the inner structure of cuticles and carbonaceous compressions using Early Jurassic fossil plant remains from Argentinian Patagonia, as an example of application to plant macrofossils.

## Material and methods

### *Provenance and characteristics of the studied materials*

The studied material consists of two fragments of conifer leafy twigs preserved as cutinised compressions from Early-Middle Jurassic lacustrine deposits of the Cañadón Asfalto Formation in central Patagonia, Argentina (Cúneo *et al.*, 2013; Figari *et al.*, 2015). These leafy twigs have rhomboidal scale-like leaves, very tightly disposed on the axis, with papillate scarios margins, and very abundant epidermic papillae concentrated on the leaf base and margins (Fig. 1). The leaves are amphystomatic with monocyclic stomatal apparatuses randomly oriented, with 5–6 subsidiary cells per stomata, all of them presenting a single papilla oriented towards the sunken stomatal aperture.

### *Sample preparation, work methodology and FIB-SEM experimental parameters*

We performed the analysis at the Electron Microscopy Service (CACTI) (<http://cactiweb.webs.uvigo.es/Joomla/index.php>) of the University of Vigo (Pontevedra, Spain). Observations were performed using an FEI Helios G1 600 (Oregon, USA) Nanolab equipped with a field emission gun (FEG) and multiple electron detectors for image acquisition, including a through-lens detector (TLD), an Everhart–Thornley detector (ETD) and a back scattered electron detector (BSED) for compositional information.

FIB-SEM is an analytical technique based on the unique combination of an ion gun and an electron gun, which permits

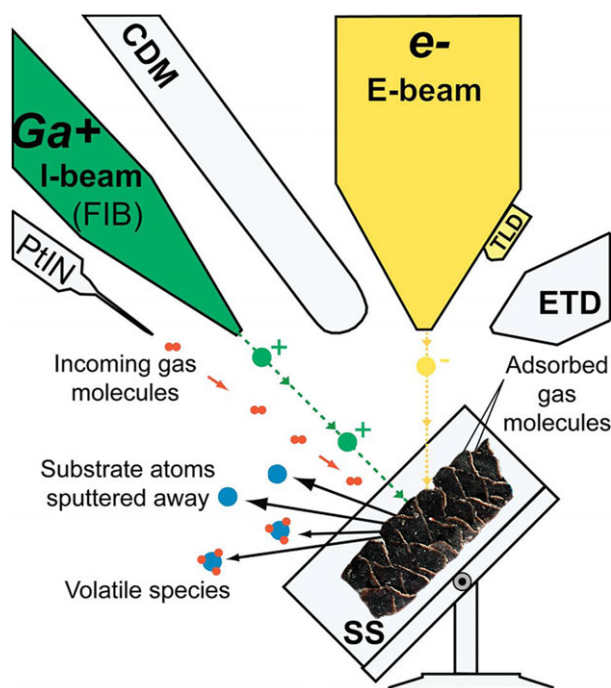


Fig. 1. Schematic diagram of the FIB-SEM device and its operating mode. Everhart–Thornley detector; PtIN, platinum injection needle; SS, sample stage; CDM, continuous dynode electron multiplier detector; ETD, Everhart–Thornley detector; TLD, through-lens detector. (Modified from Villanueva-Amadoz *et al.*, 2012.).

simultaneous sectioning and electron imaging of the region of interest with a spatial resolution within the 10 nm range.

For a more detailed description on the fundamentals of this technique see Orloff *et al.* (2003), Giannuzzi & Stevie (2005) and Volkert & Minor (2007).

Even though no previous chemical treatment is required, we suggest a basic cleaning of the cuticle with HF or/and HCL. This will decrease milling time by eliminating the rock matrix and excess surface debris (Figs. 2B–D).

The fossil samples were mounted on a SEM stub and then coated with a thin (~20 nm) gold layer to make them conductive. The sample stage was tilted at 52° from the horizontal position (Fig. 1), to ensure the sample surface is perpendicular to the gallium ion beam

We employed an ion current of 9.3 nA at 30 kV acceleration voltage to mill a trench of 100 μm in length, 30 μm in width and 50 μm in depth. Despite using the second highest beam current available, this first rough cut required a few hours. The vertical surface of the trench was then polished using the ‘cleaning cross-section option’, in which the ion beam is rastered in slices parallel to the surface of the cut (i.e. perpendicular to the sample surface). An initial current of 2.8 nA was used, followed by an intermediate current of 0.42 nA. Finally, the use of a low (93 pA) current allowed a fine polishing of a selected portion of the sectioned region. The total process took approximately 8–10 h.

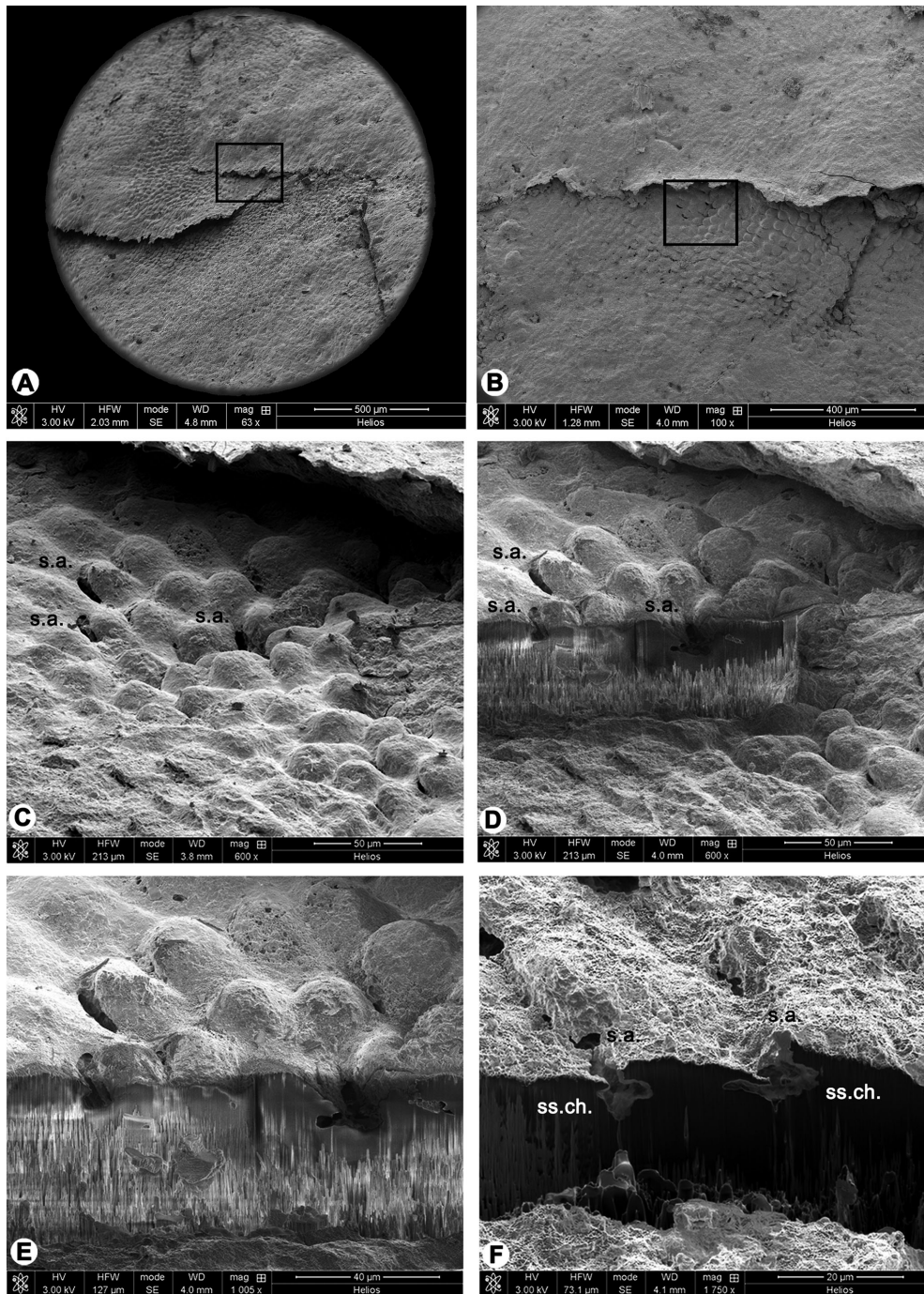


**Fig. 2.** Images showing the process of cutting and milling of a leaf compression corresponding to a fossil conifer showing their internal structures. (A) View of several scale-like shaped leaves corresponding to the leafy branch of conifer of the Early Middle Jurassic from Argentinian Patagonia that was disposed in the stub in Figure 1. The rectangular frame indicates the area that was selected to develop the study. (B) Selected area in A corresponding to the contact between two leaves. Stomatal apertures can be seen as tiny black holes in the central zone of the framed area. (C) External surface of the cuticle – framed area in B – corresponding to the base of a fossil leaf of conifer, which is covered by epidermal papillae showing several stomatal apertures. (D) Cross-sectional image of the same zone as in C. (E) Detail of the same section in D showing process induced ‘stalactitic’ structures. (F) The same zone as in E but without the ‘stalactitic’ structures, going deeper inside the compression due to the more advanced milling process Initials corresponding to the working conditions (placed in the black bar at the base of images): HV, voltage; HFW, range of the image display; WD, working distance; mag, magnification. Abbreviations of features indicated in the images: s.a., stomatal aperture; ss.ch., substomatic chamber.

A relevant difficulty during the processing with FIB usually is the redeposition of the milled material, particularly when high currents are used (Villanueva-Amadoz *et al.*, 2012). It has been suggested that this effect can be potentially reduced by the use of Selective Carbon Etching (SCE), which consists of injecting water vapour (as magnesium sulphate hepta-hydrate) during ion milling; in this way, the milling rate is considerably increased, consequently reducing the redeposition effects. Nonetheless, in this study, the use of SCE did not produce the intended effect and some 'stalactite-shaped' structures appeared in front of the cut surface (Figs. 2B, C, E). X-ray analysis revealed them to be composed essentially of gallium. A possible explanation for this counter-intuitive behaviour could lie on the extremely dis-homogenous composition of the fossil cuticle, and hence in the highly variable density of the specimens, where carbon-based material is usually mixed with clastic particles. This may result in a very fast milling of the 'soft' matrix leaving remains of much more resistant rocky matrix on which the gallium redeposits. We therefore carried out a systematic analysis to optimise the milling parameters and finally decided not to use the SCE system. In relation to the possible redeposition of gallium on the sample, X-ray analysis showed that the rims of sectioned cavities contain a relevant amount of gallium on average, indicating that structures in those areas must be considered, at least partly, as process induced artefacts. Redeposition also occurs inside the cavities. Nevertheless, due to the very low percentage of gallium present there we consider that both micro and ultrastructures visible in these areas are not artefacts but real structures merely covered by an extremely thin layer of gallium (Figs. 5, 6).

The formation of Ga-rich artefacts can be partially reduced by lowering the ion current used for the final polishing. Figure 4(C) shows a cavity after final polishing at 46 pA ion current, and it can be seen as the Ga-rich bright layer surrounding the cavity reduced in size but did not disappear; however, a lower current implies a much longer milling time, rendering the whole setup impractical.

We also checked the option of covering a part of the sample with platinum – following the standard first step in the FIB milling procedure – in order to protect the material before the milling process to prevent redeposition of both gallium and debris. Nevertheless, in the case of a region with cavities was to fill the cavity with this metallic element, which altered its composition and morphology. Moreover, only a broken and discontinuous strip was deposited over both the studied surfaces and sections, which impeded the observations of the sample. Therefore, no platinum strip was deposited here.

Images were acquired using the TLD for secondary electrons, enabling us to work with a spatial resolution within the 10 nm range. As the final cleaning process is extremely slow due to the very low (93 pA) current employed, we carefully cleaned only selected regions of the original cut corresponding to those areas close to the stomatal openings (Figs. 2F, 3A–F, 4A–F).

## Results

The FIB-SEM technique allowed us to observe and identify a number of internal and external cuticular micro/ultrastructures, some of which have never been previously reported for any type of fossil cuticles.

### Microstructures

**Internal cavities.** Internal cavities were identified after sectioning the stomatal apparatuses. These sections affected the epidermal papillae that surround stomata and subsidiary cells (Fig. 2). A series of cavities of 17  $\mu\text{m}$  maximum length/width can be seen in the section tens of microns below the cuticle surface reaching carbonised epidermic layers, which, due to their morphology and location, may represent substomatic chambers. These cavities occur in the inner part of the foliar epidermis and appear to be filled with carbonaceous matter, which has been corroborated via several elemental spectrums by means of X-ray analysis (Fig. 5). They are preserved unmodified due to the exceptional conditions within the rock matrix, probably favoured by its very fine-grained nature. Likely, these plant remains were rapidly buried in an anoxic environment, allowing cuticles and other foliar tissues to be exceptionally preserved and retaining their structural integrity without any perceptible deformation (Figs. 2E, F, 3A, E, 4C, D). We find that the shape and size of these cavities varies as the milling process advances into the carbonaceous compression.

**Internal microtunnels:** Tiny holes, 2.5  $\mu\text{m}$  to 800 nm in diameter, were observed inside the internal cavities. The milling process shows that these holes penetrate inside the sample through the cavity and are orientated perpendicular to the stomatal aperture, as such they could be considered as small tunnels placed into the major cavity (Figs. 4A, B).

**Associated microcharacterisation:** The internal side of the cavity walls represent a sort of 'carbon-copy' of epidermal cells (Figs. 3A, B, 3D, E, 4A, B), not fully defined due to the coalification process. Square to rectangular-shaped micromorphologies are occasionally observed on the walls of the cavities, which could correspond to epidermal cells (Fig. 3F).

**Ultrastructures.** We identified a number of ultrastructures within the hollow spaces and cavities described above, including:

**Scale-like structures:** based on their location in the external part of the cuticle, their morphology and imbrication, these scale-like ultrastructures (60 nm long and 40 nm wide in average) are interpreted as epicuticular wax (Fig. 4E).

**Depressions:** circular or elliptic shallow ultrastructures 800 nm in diameter on average, showing tapering towards the base and sides of the cavities (Fig. 3B)

**Circular perforations:** they range from 200 nm to 300 nm in diameter and locate at the base of the internal cavities (Fig. 3C).

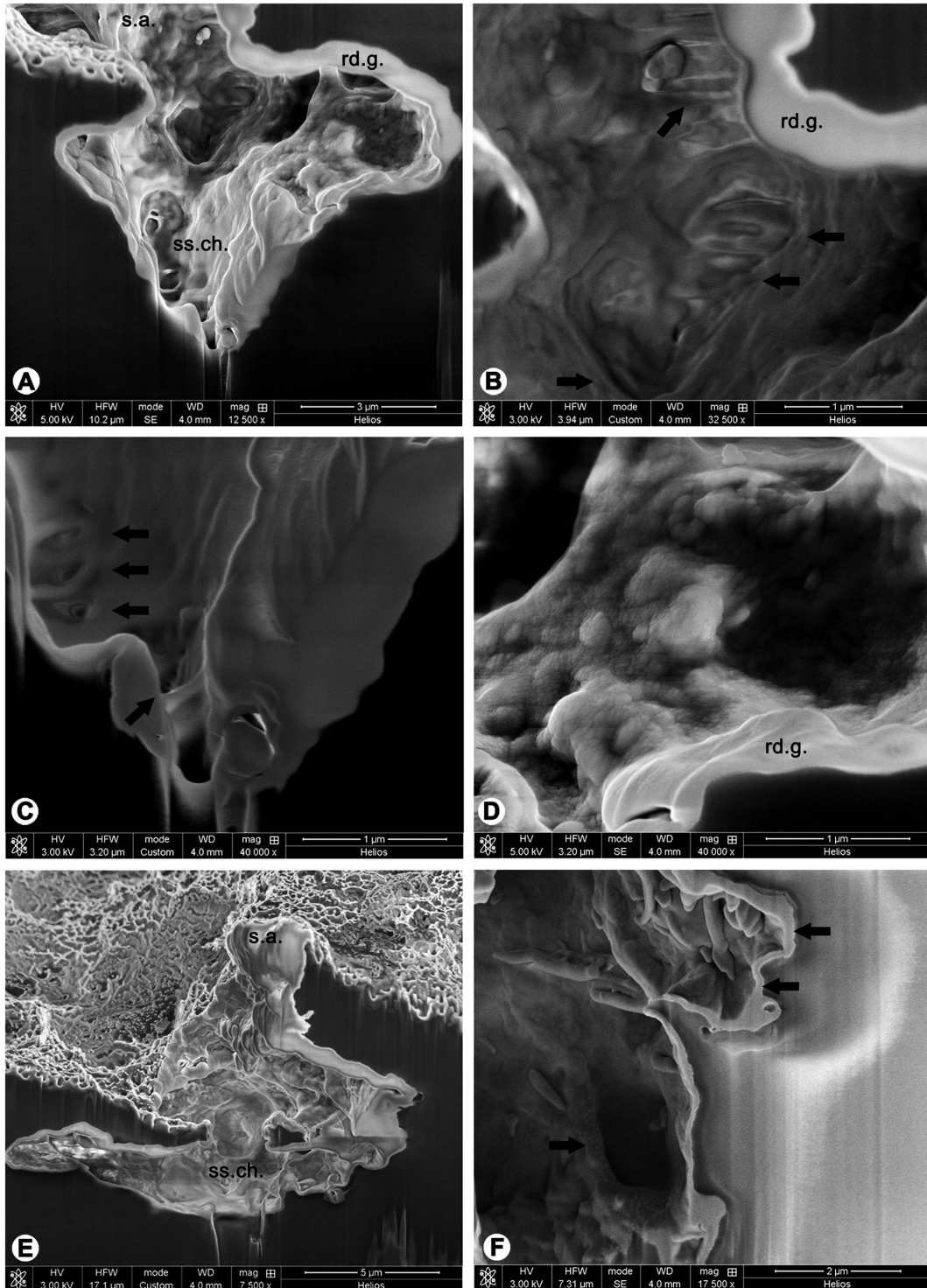


**Fig. 3.** Images of the internal chambers and higher magnification details of the same regions in Figure 2. (A) Internal cavity (substomatic chamber) showing several structures. (B) Detail of the upper part of A showing several ultrastructural depressions and circular perforations in the inner wall of the chamber (black arrows). (C) Detail of the lower part of A showing ultrastructural circular perforations and channels at the base of the cavity (black arrows). (D) Detail of the right side of A showing the inner part of the chamber wall, which presents several protuberances and a grainy texture. (E) Another substomatic chamber in section. (F) Detail of image E that shows the rectangular-shaped micromorphologies of the wall of the substomatic chamber (black arrows) that is adapted probably to the morphology of the external parts of the epidermal cells. Abbreviations of features indicated in the images: s.a., stomatal aperture; ss.ch., substomatic chamber; rd.g., redeposited gallium structure.

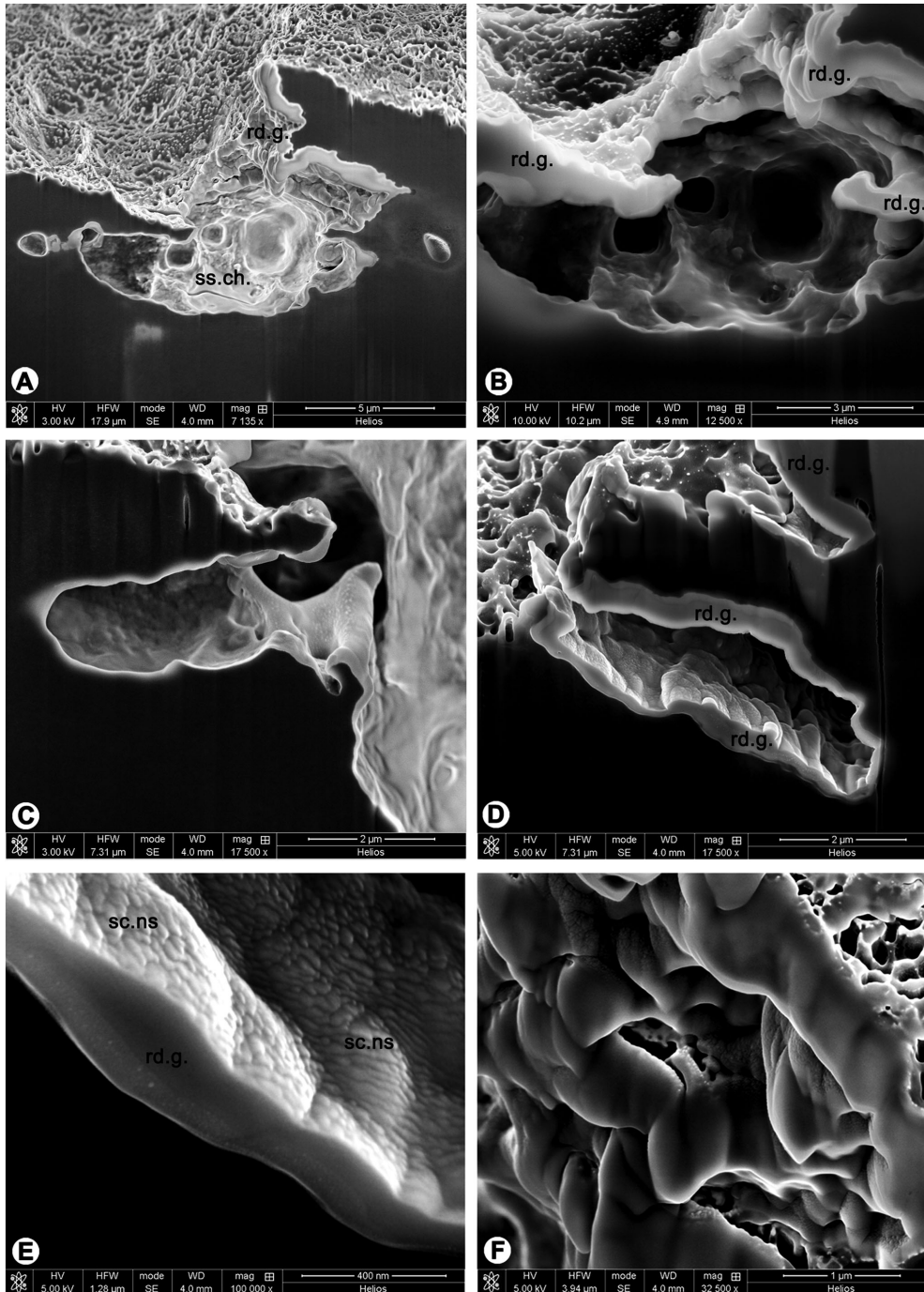
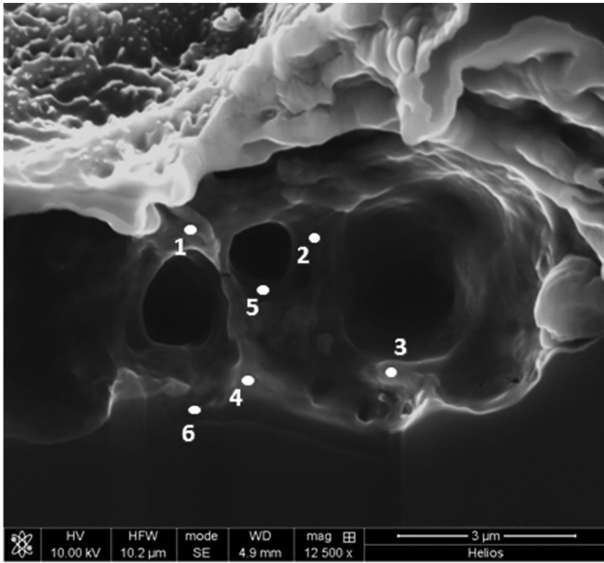


**Fig. 4.** Details of the internal chambers and redeposited gallium structures. (A) View of a section in the initial stages of the milling process corresponding to another substomatic chamber. (B) Detail of the central region of A in a posterior stage of the milling process showing scarce redeposition of gallium in the inner parts of the substomatic chamber. Tunnel-like structures penetrating the substomatic chamber can be seen as dark holes. (C) Cavity after polishing at 46 pA ion current. The Ga-rich is clearly identifiable as a bright layer surrounding the cavity. (D) External cavity composed by the folding of the epidermal tissue. The corrugated structure of the upper surface of the folding part inside the cavity is visible as it is the carbonaceous compression of lower tissues (black matter). The bright fringe surrounding the cavity corresponds to redeposition of gallium. (E) Detail of the left part of D, showing the presence of scale-like, nanometre-sized ultrastructures on the internal part of the cavity. The white-coloured fringe on the edge of the cavity corresponds to Ga redeposition. (F) Detail of the central-right region on A showing structures as folds and convolutions partly covered by redeposited gallium. Abbreviations of features indicated in the images: ss.ch., substomatic chamber; sc.ns., scale-like nanostructures; rd.g., redeposited gallium-forming structure.



Spect	C	O	Mg	Si	S	Ca	Ga
1	56.90	19.28		2.26	3.61	10.78	7.18
2	56.29	9.40			9.78	20.65	3.88
3	42.10	27.29		1.74	5.57	11.53	11.7
4	59.38	33.50	1.10		1.27	2.45	2.29
5	65.66				10.54	20.89	2.91
6	72.02	22.27	0.66	0.35	1.98	2.04	0.68

Fig. 5. Elemental composition inside the cavity in Figure 4(B). Concentrations are given in atomic percentage, with an estimated relative error of ±1%.

**Channels:** they can be observed in transversal sections 300–500 nm wide at the cavity base and associate with circular perforations (Fig. 3C).

**Granular bodies:** small hemispherical ultrastructures that appear to be associated to cavity surfaces (Fig. 3D).

*Artificial structures created by redeposition*

Due to the milling process some of the gallium was redeposited on the sectioned walls creating some artificial artefacts that do not represent the original structure of the fossil material

**Microlayers:** layers of different thicknesses partly composed of redeposited gallium were detected in some regions covering the rim of the section of internal cavities (Figs. 3A, B, D, F).

**Foldings and convolutions:** wrinkly textures approximately 1 μm in width and several μm in length – partly composed of redeposited gallium – occur on the external side of the cavities (Figs. 3A, E, 4A, F).

**Discussion**

*Comparative advantages of the FIB-SEM technique*

The FIB-SEM technique has proven itself extremely useful in ultrastructural studies of various biological materials (Nalla *et al.*, 2005; House & Balkwill, 2013 and references therein), allowing for the *in situ* observation of previously unobserved features. Compared to other scanning electron or X-ray volume imaging techniques, FIB-SEM systems typically have very high imaging resolution and allow for direct observation of near-subsurface structures. However, its main application in palaeontology so far has been preparing ultrathin lamellas for observation by conventional SEM or, more commonly, TEM (Kempe *et al.*, 2005; Wacey *et al.*, 2012), and has been rarely

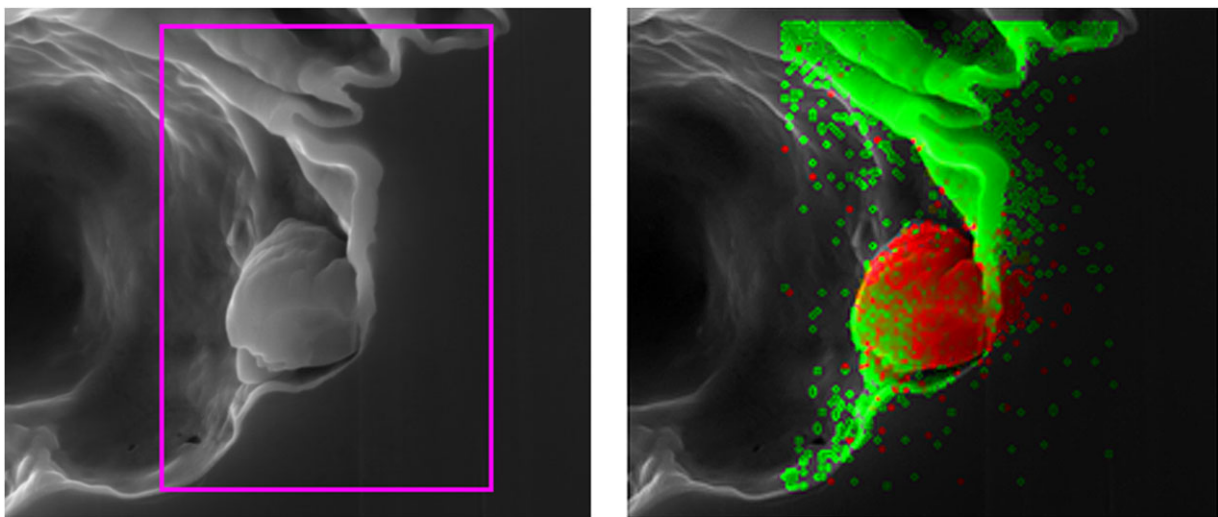


Fig. 6. Gallium elemental map compared with another element present (Silicon) in the sectioned region corresponding to one of the inner chambers (framed area). The distribution of both elements is plotted in the map (Gallium in green and Silicon in red). Scale bar: 2 μm

used to directly observe the internal structure after ion-milling slicing (Schiffbauer & Xiao, 2009, 2011; Pang *et al.*, 2013; Brasier *et al.*, 2015).

An additional advantage of using FIB-SEM on fossil plants is the possibility to precisely choose the feature of interest, slice it and analyse it within the same instrument, thus reducing the number of processing steps and increasing time and cost efficiencies.

We have shown here the possibility of obtaining direct three-dimensional information from combined surface and subsurface cross-sectional views of these fossil cuticles, internal cavities and coalified tissues, all with little to no time consuming sample preparation. Despite being a destructive technique, FIB-SEM results are clearly more useful than any 2D light microscopy image, allowing the observation of both micro- and ultrastructural features (Villanueva-Amadoz *et al.*, 2012). Furthermore, FIB-SEM allows for precise site-specific subsurface analysis, as compared to other methods like fracturing or mechanical sectioning. Finally, sequential ion milling following by image reconstruction may be used to better visualise in three dimensions the subsurface structures (e.g. Schiffbauer & Xiao, 2009).

TEM has been widely used to study details such as structure and disposition of the cell walls, stomatal openings or organisation of papillae and guard cells (Guignard *et al.*, 1998; Zhou *et al.*, 2000; Gomez *et al.*, 2002, 2012; Nosova & Wcislo-Luranc, 2007; Yang *et al.*, 2009 among other authors), providing detailed information on cuticle multilayering and ultrastructure (Guignard *et al.*, 1998, 2004). Nevertheless, the FIB-SEM technique represents an improvement when analysing plant fossil compressions, because it not only allows viewing the sample surface at the same time as the vertical surface of the cut but it also makes possible to both control and modify the direction of the cut at any time during the process.

When compared to synchrotron X-ray microtomography, a more recent and nondestructive technology, FIB-SEM provides direct 3D images with four times higher resolution (Cunningham *et al.*, 2014), it is generally less time-consuming (depending on the dimensions of the trench in the cut), and it implies much lower costs and less sophisticated software tools, not to mention the higher number of FIB-SEM instruments available.

In summary, when compared with other microscopic methods to study fossil cuticles this technique offers very high imaging resolution (~10 nm) throughout a complete structure without any previous preparation nor subsequent software data treatment. Moreover, only a trench few tens of microns long, wide and deep is necessary, with minimal sample damage outside of the milled region.

#### *FIB-SEM particular usefulness in the study of fossil cuticles*

The technique has allows to observation of microcharacteristics contained in the cuticle ultrastructure as well as

micromorphologies such as cavities located on coalified epidermal tissues of fossil cuticles. In this respect, standard techniques preclude the preservation of coaly materials in order to make cuticles clean to study (e.g. Kerp, 1990; Guignard *et al.*, 1998; Yang *et al.*, 2009).

The identification of microcavities in 3D that could represent substomatal chambers, previously only reported in rare cases (e.g. Edwards, 2003), represents the first time that they are observed in fossil coalified compressions. Because stomatal chambers have an important role in the exchange of gases in leaves, this new methodology might allow now to proceed with additional interpretations associated to palaeoenvironmental and palaeoclimatic parameters. Thus, newly the identification of microstructures at the ultrastructural level in fossil compressions might contribute with new data that could be an additional factor in the studies and interpretation of CO<sub>2</sub> distribution in the past. In addition, this technique allows to obtain an estimated value of the volume of these chambers through the application of tomographic sequential milling (Schiffbauer & Xiao, 2011; Brasier *et al.*, 2015).

These new data open a variety of possibilities in the comparative study of different inner structures implicated in the exchange of gases in fossil plants and their relationships with the number of stomatal apparatuses in the surface of leaves. However, as it is the first time that this technique is applied in fossil leaves, we cannot speculate on the plasticity or even the variability of these features. Thus, it becomes essential to further investigate this field by analysing modern plants and then try to extrapolate results performing more experiments in new fossil specimens.

Finally, the characterisation of number, distribution and morphology of micro- and nano-ornamentations in the substomatal chamber, could provide important results in terms of identifying new characters of systematic importance, that is, disposition, morphology and ornamentation of the different micrometrical structures present in the walls of the substomatal chambers. This could be corroborated by analysing with FIB-SEM a large number and a variety of current and fossil leaves of different plant groups.

#### **Conclusions**

FIB-SEM analysis of fossil plant remains opens new possibilities in terms of identifying and observing microstructures, something previously only possible by using more time-consuming and expensive methodologies, that is TEM or synchrotron X-ray tomography. The technique does not require any complex sample preparation, it is almost directly applicable, and it has proven extremely successful in terms of identifying nanometric microstructures in fossil cuticles. For the first time it has been possible to observe subcuticular coalified cavities that closely resemble substomatal chambers and their associated microstructures with a spatial resolution within the tens of nanometre range. This analytical technique to



observe and identify cuticular and subcuticular nano- and microstructures, result more accessible and cost efficient than the conventional ones, and yields higher quality information, which can be profitably applied to different disciplines including palaeoenvironmental, palaeoclimate and, likely, taxonomic/phylogenetic approaches.

During the development of this technique in coalified plant fossil compressions some pitfalls were identified by X-ray analysis as growing of stalactitic structures or redeposition of gallium over the surfaces. Nevertheless, the use of an adequate milling voltage allowed a nearly complete elimination of the process induced artefacts. This corroborate our theory that the ornamentations on surfaces are original and not artefacts, despite that the fact that the origin of the smallest irregular-shaped scale-like nanostructures remains uncertain due to their extremely reduced size.

The possibility of identifying rarely preserved microstructures like substomatal chambers, for instance, supply reliable autecological information not previously available and allows a close comparison with results obtained by classical methodologies. Therefore, it becomes important to apply it to modern plants, which should provide additional evidence of the presence of similar microstructures in fossil remains, as well as supply data on the morphological plasticity of these structures.

### Acknowledgements

The authors thank to Mr. Eduardo Ruigomez 'Dudu' – curator of Museo Paleontológico Egidio Feruglio from Trelew (Chubut province, Argentina) – for his help and for his disposition to the accessibility of the studied material. We also thank the comments and indications of the two anonymous referees, which have improved notably this manuscript. This article is a contribution to project PICT 2012 N° 1520 of the 'Agencia Nacional de Promoción Científica y Tecnológica' from the 'Ministerio de Ciencia y Tecnología e Innovación Productiva' of the Argentinian Republic Government.

### References

- Alvin, K.L. (1970) The study of fossil leaves by SEM. In *Proceedings of the Third Annual Scanning Electron Microscope Symposium*. pp. 121–128. IIT Research Institute, Chicago.
- Archangelsky, S., Taylor, T.N. & Kurmann, M.H. (1986) Ultrastructural studies of fossil plant cuticles: *Ticoa harrisii* from the Early Cretaceous of Argentina. *Bot. J. Linn. Soc.* **92**(2), 101–116.
- Bernard, S., Benzerara, K., Beyssac, O., Menguy, N., Guyot, F., Brown, G.E. & Goffe, B. (2007) Exceptional preservation of fossil plants spores in high-pressure metamorphic rocks. *Earth Planet. Sci. Lett.* **262**, 257–272.
- Bhawana, Miller, J.L. & Cahoon, A.B. (2014) 3D Plant cell architecture of *Arabidopsis thaliana* (Brassicaceae) using focused ion beam–scanning electron microscopy. *Applications in Plant Sciences*, **2**(6), 1300090. <https://doi.org/10.3732/apps.1300090>
- Brasier, M.D., Antcliffe, J., Saunders, M. & Wacey, D. (2015) Changing the picture of Earth's earliest fossils (3.5–1.9 Ga) with new approaches and new discoveries. *Proc. Nat. Acad. Sci. U.S.A.* **112**, 4859–4864.
- Cúneo, R., Ramezani, J., Scasso, R., Pol, D., Escapa, I., Zavattieri, A.M. & Bowering, S.A. (2013) High-precision U–Pb geochronology and a new chronostratigraphy for the Cañadón Asfalto Basin, Chubut, central Patagonia: implications for terrestrial faunal and floral evolution in Jurassic. *Gondw. Res.* **24**, 1267–1275.
- Cunningham, J.A., Rahman, I.A., Lautenschlager, S., Rayfield, E.J. & Donoghue, P.C.J. (2014) A virtual world of paleontology. *Trends Ecol. Evol.* **29**(6), 347–357.
- de Winter, D.A.M., Schneijdenberg, C.T.W.M., Lebbink, M.N., Lich, B., Verkleij, A.J., Drury, M.R. & Humbel, B.M. (2009) Tomography of insulating biological and geological materials using focused ion beam (FIB) sectioning and low-kV BSE imaging. *J. Microsc.* **233**(3), 372–383.
- Drobne, D., Milani, M., Zrimec, A., Zrimec, M.B., Tatti, F. & Draslar, K. (2005) Focused ion beam/scanning electron microscopy studies of Porcellio scaber (Isopoda, Crustacea) digestive gland epithelium cells. *Scanning* **27**(1), 30–34.
- Dumont, M., Kostka, A., Sander, P.M., Borbely, A. & Kaysser-Pyzalla, A. (2011) Size and size distribution of apatite crystals in sauropod fossil bones. *Palaeogeogr., Palaeoclim., Palaeoecol.* **310**(1–2), 108–116.
- Edwards, D. (2003) Embryophytic sporophytes in the Rhynie and Windyfield cherts. *Transact. R. Soc. Edinb.: Earth Sci.* **94**, 397–410.
- Figari, E.G., Scasso, R.A., Cúneo, R.N. & Escapa, I. (2015) Estratigrafía y evolución geológica de la Cuenca de Cañadón Asfalto, Provincia del Chubut, Argentina. *Latin Am. J. Sediment. Basin Anal.* **22**(2), 135–169.
- Florin, R. (1933) Studien Über die Cycadales des Mesozoikums nebst Erörterungen über die Spaltöffnungsapparate der Bennettitales. *Kungl. Sven. Vetenskapsak. Handl. (ser. 3)*, **12**(5), 1–134.
- Fujii, T. & Kaito, T. (2005) Nano factory achieved by focused ion beam. *Microsc. Microanal.* **11**(Suppl 2), 810–811.
- Giannuzzi, L.A. & Stevie, F.A. (2005) *Introduction to Focused Ion Beams: Instrumentation, Theory, Techniques and Practice*. Springer, New York.
- Gomez, B., Martín-Closas, C., Barale, G., Solé de Porta, N., Thévenard, F. & Guignard, G. (2002) Frenelopsis (Coniferales: Cheirolepidiaceae) and related male organ genera from the lower Cretaceous of Spain. *Palaeontology* **45**(5), 997–1036.
- Gomez, B., Ewin, T.A.M. & Daviero-Gomez, V. (2012) The conifer *Glenrosa falcata* sp. nov. from the Lower Cretaceous of Spain and its palaeoecology. *Rev. Palaeobot. Palynol.* **172**, 21–32.
- Grandfield, K. & Engqvist, H. (2012) Focused ion beam in the study of biomaterials and biological matter. *Adv. Mater. Sci. Eng.*, Article ID 841961, 1–6.
- Guignard, G., Thévenard, F. & van Konijnenburg-van Cittert, J.H.A. (1998) Cuticle ultrastructure of the cheirolepidiaceae conifer *Hirmeriella muensteri* (Schenk) Jung. *Rev. Palaeobot. Palynol.* **104**, 115–141.
- Guignard, G., Popa, M.E. & Barale, G. (2004) Ultrastructure of Early Jurassic fossil plant cuticles: *Pachypteris gradinarui* Popa. *Tissue Cell* **36**, 263–273.
- Harris, T.M. (1979) *The Yorkshire Jurassic Flora V. Coniferales*. British Museum (Natural History), London, 167 pp.
- Haworth, M. & McElwain, J.C. (2008) Hot, dry, wet, cold or toxic? Revisiting the ecological significance of leaf and cuticular micromorphology. *Palaeogeogr., Palaeoclim., Palaeoecol.*, **262**, 79–90.

- Haworth, M., Hesselbo, S.P., McElwain, J.C., Robinson, S.A. & Brunt, J.W. (2005) Mid-Cretaceous pCO<sub>2</sub> based on stomata of the extinct conifer *Pseudofrenelopsis* (Cheirolepidiaceae). *Geology* **33**, 749–752.
- Haworth, M., Elliott-Kingston, C. & McElwain, J.C. (2011) Stomatal control as a driver of plant evolution. *J. Exp. Bot.* **62**(8), 2419–2423.
- Heaney, P.J., Vicenzi, E.P., Giannuzzi, L.A. & Livi, K.J.T. (2001) Focused ion beam milling: a method of site-specific sample extraction for micro-analysis of earth and planetary materials. *Am. Miner.* **86**, 1094–1099.
- Hoffmann, R., Kirchlechner, C., Langer, G., Wochnik, A.S., Griesshaber, E., Schmahl, W.W. & Scheu, C. (2015) Insight into *Emiliana huxleyi* coccospheres by focused ion beam sectioning. *Biogeosciences* **12**, 825–834.
- House, A. & Balkwill, K. (2013) FIB-SEM: an additional technique for investigating internal structure of pollen walls. *Microsc. Microanal.* **19**(06), 1535–1541.
- Javed, H., Saddiqi, N.H. & Islam, M. (2014) Recent advancements in focused ion beam applications: a review. *Int. J. Recent Sci. Res.* **5**(1), 123–127.
- Kempe, A., Wirth, R., Altermann, W., Stark, R.W., Schopf, J.W. & Heckl, W.M. (2005) Focused ion beam preparation and in situ nanoscopic study of Precambrian acritarchs. *Precamb. Res.* **140**, 36–54.
- Kerp, H. (1990) The study of fossil gymnosperms by means of cuticular analysis. *Palaïos* **5**, 548–569.
- Krings, M. (2000) The use of biological stains in the analysis of late Palaeozoic pteridosperm cuticles. *Rev. Palaeobot. Palynol.* **108**, 143–150.
- Lee, M.R., Bland, P.A. & Graham, G. (2003) Preparation of TEM samples by focused ion beam (FIB) techniques: applications to the study of clays and phyllosilicates in meteorites. *Miner. Magaz.* **67**, 581–592.
- Marko, M. (2010) Focused ion beam applications in biology. *Microsc. Microanal.* **16**, 1944–1945.
- McElwain, J.C. (1998) Do fossil plants signal palaeoatmospheric CO<sub>2</sub> concentration in the geological past? *Philos. Transact. R. Soc. Lond. B* **353**, 83–96.
- McElwain, J.C. & Chaloner, W.G. (1996) The fossil cuticle as a skeletal record of environmental change. *Palaïos* **11**, 376–388.
- McElwain, J.C. & Chaloner, W.G. (1995) Stomatal density and index of fossil plants track atmospheric carbon dioxide in the Palaeozoic. *Ann. Bot.* **76**, 389–395.
- Milani, M., Drobne, D. & Tatti, F. (2007) How to study biological samples by FIB/SEM? *Modern Research and Educational Topics in Microscopy* (ed. by A. Méndez-Vilas and J. Díaz), pp. 787–794. Formatex Research Center Publishing, Badajoz, Spain.
- Milani, M., Gottardi, R., Savoia, C. & Cattaneo, C. (2012) FIB/SEM/EDS complementary analysis for proper forensic interpretation. *Current Microscopy Contributions to Advances in Science and Technology* (ed. by A. Méndez-Vilas), pp. 179–185. Formatex Research Center Publishing, Badajoz, Spain.
- Moberly, C., Warren J., Adams, D.P., Aziz, M.J., Hobler, G. & Schenkel, T. (2007) Fundamentals of focused ion beam nanostructural processing: below, at, and above the surface. *MRS Bull.* **32**(5), 424–432.
- Möslé, B., Collinson, M E, Finch, P., Stankiewicz, B.A., Scott, A.C. & Wilson, R. (1998) Factors influencing the preservation of plant cuticles: a comparison of morphology and chemical composition of modern and fossil examples. *Org. Geochem.* **29**(5–7), 1369–1380.
- Nalla, R.K., Porter A.E, Daraio, C., Minor, A.M., Radmilovic, V., Stach, E.A., Tomsia, A.P. & Ritchie, R.O. (2005) Ultrastructural examination of dentin using focused ion-beam cross-sectioning and transmission electron microscopy. *Micron* **36**(7–8), 672–680.
- Nguyen Tu, T.T., Bocherens, H., Mariotti, A., Baudin, F., Pons, D., Broutin, J., Derenne, S. & Largeau, C. (1999) Ecological distribution of Cenomanian terrestrial plants based on 13C/12C ratios. *Palaeogeogr., Palaeoclim., Palaeoecol.* **145**, 79–93.
- Nosova, N. & Wcislo-Lurancic, E. (2007) A reinterpretation of *Mirovia* *Reymanówna* (Coniferales) based on the reconsideration of the type species *Mirovia saferi* *Reymanówna* from the Polish Jurassic. *Acta Palaeobotanica* **47**(2), 359–377.
- Orloff, J., Utlaut, M. & Swanson, L. (2003) *High Resolution Focused Ion Beams: FIB and Its Applications*. Kluwer Academic/Plenum Publishers, New York.
- Orso, S. (2005) Structural and mechanical investigations of biological materials using a Focussed Ion Beam microscope. PhD Thesis dissertation, Institut für Metallkunde. Max-Planck-Inst. für Metallforschung (Stuttgart), 172 pp.
- Pang, K., Tang, Q., Schiffbauer, J.D. *et al.* (2013) The nature and origin of nucleus-like intracellular inclusions in Paleoproterozoic eukaryote microfossils. *Geobiology* **11**, 499–510.
- Rigort, A., Bäuerlein, F.J.B., Villa, E., Eibauer, M., Laugks, T., Baumeister, W. & Plitzko, J.M. (2012) Focused ion beam micromachining of eukaryotic cells for cryoelectron tomography. *Proc. Nat. Acad. Sci. U.S.A.* **109**(12), 4449–4454.
- Royer, D.L. (2001) Stomatal density and stomatal index as indicators of paleoatmospheric CO<sub>2</sub> concentration. *Rev. Palaeobot. Palynol.* **114**, 1–28.
- Royer, D.L. (2008) Linkages between CO<sub>2</sub>, climate, and evolution in deep time. *Proc. Nat. Acad. Sci. U.S.A.* **105**, 407–408.
- Santschi, C., Przybylska, J., Guillaumee, M., Vazquez-Mena, O., Brugger, J. & Martin, O.J.F. (2009) Focused ion beam: a versatile technique for the fabrication of nano-devices. *Praktis. Metallogr.* **46**, 154–156.
- Schiffbauer, J. D. & Xiao, S. (2009) Novel application of focused ion beam electron microscopy (FIB-EM) in the preparation and analysis of microfossil ultrastructures. *Palaïos* **24**, 616–626.
- Schiffbauer, J.D. & Xiao, S. (2011) Paleobiological applications of focused ion beam electron microscopy (FIB-EM): an ultrastructural approach to the (micro)fossil record. *Quantifying the Evolution of Early Life: Numerical Approaches to the Evaluation of Fossils and Ancient Ecosystems* (ed. by M. Laflamme), pp. 321–354. Springer, New York.
- Spicer, R.A. & Thomas, B.A. (eds.) (1986) *Systematic and Taxonomic Approaches in Paleobotany*. Systematics Association Special Volume 31. Oxford University Press, New York.
- Sreelakshmi, V.V, Sruthy, E.P.M. & Shereena, J. (2014) Relationship between the leaf area and taxonomic importance of foliar stomata. *Int. J. Res. Appl., Nat. Soc. Sci.* **2**(7), 53–60.
- Steinhorsdottir, M. & Vajda, V. (2015) Early Jurassic (late Pliensbachian) CO<sub>2</sub> concentrations based on stomatal analysis of fossil conifer leaves from eastern Australia. *Gondw. Res.* **27**(3), 932–939.
- Steinhorsdottir, M., Jeram, A.J. & McElwain, J.C. (2011) Extremely elevated CO<sub>2</sub> concentrations at the Triassic/Jurassic boundary. *Palaeogeogr., Palaeoclim., Palaeoecol.* **308**, 418–432.
- Stockey, R.A. (1994) Mesozoic araucariaceae: morphology and systematic relationships. *J. Plant Res.* **107**, 493–502.
- Stokes, D.J. & Hayles, M.F. (2009) Methodologies for the preparation of soft materials using CryoFIB SEM. *Proceed. SPIE* **7378**, 1–12.
- Taylor, T.N., Taylor, E.L. & Krings, M. (2009) *The Biology and Evolution of Fossil Plants*. 2nd edn., pp. 1230. Academic Press, Amsterdam.

- Tosolini, A.M.P., McLoughlin, S., Wagstaff, B.E., Cantrill, D.J. & Gallagher, S.J. (2015) Cheirolepidiacean foliage and pollen from Cretaceous high-latitudes of southeastern Australia. *Gondw. Res.* **27**(3), 960–977.
- Van Gijzel, P. (1977) Die fluoreszenz-mikroskopie einiger pflanzen fossilien. *Cour. Forschungsin. Sencken.* **24**, 92–100.
- Villanueva-Amadoz, U., Benedetti, A., Mendez, J., Sender, L.M. & Diez, J.B. (2012) Focused ion beam nano-sectioning and imaging: A new method in characterisation of palaeopalynological remains. *Grana* **51**, 1–9.
- Villanueva-Amadoz, U., Estevez-Gallardo, P. & Diez, J.B. (2014) New contributions of the ultrastructure of Classopollis using FIB-SEM technique. *IX European Palaeobotany and Palynology Conference, Abstracts Book*, 298–299 (ed. by Martinetto, E., Roghi, G. and Kustatscher, E.), pp. 26–31. Museum of Nature South Tyrol, Padova (Italy).
- Vitek, N.S., Vinther, J., Schiffbauer, J.D., Briggs, D.E.G. & Prum, R.O. (2013) Exceptional three-dimensional preservation and coloration of an originally iridescent fossil feather from the Middle Eocene Messel Oil Shale. *Paläontologische Zeitschrift* **87**, 493–503.
- Volkert, C.A. & Minor, A.M. (Guest Editors). (2007) Focused ion beam: microscopy and micromachining. *Mater. Res. Soc. Bull.* **32**, 389–399.
- Wacey, D., Menon, S., Green, L., Gerstmann, D., Kong, C., McLoughlin, N., Saunders, M. & Brasier, M. (2012) Taphonomy of very ancient microfossils from the ~3400 Strelley Pool Formation and ~1900 Ma Gunflint formation: New insights using a focused ion beam. *Precamb. Res.* **220–221**, 234–250.
- Wagenknecht, T., Hsieh, C. & Marko, M. (2015) Skeletal muscle triad junction ultrastructure by focused-ion-beam milling of muscle and cryo-electron tomography. *Eur. J. Transl. Myol.* **25**, (1), 49–56.
- Wirth, R. (2004) Focused ion beam (FIB): a novel technology for advanced application of micro- and nanoanalysis in geosciences and applied mineralogy. *Eur. J. Miner.* **16**, 863–876.
- Yang, X., Guignard, G., Thevenard, F., Wang, Y. & Barale, G. (2009) Leaf cuticle ultrastructure of *Pseudofrenelopsis dalatzensis* (Chow et Tsao) Cao ex Zhou (Cheirolepidiaceae) from the Lower Cretaceous Dalazi Formation of Jilin, China. *Rev. Palaeobot. Palynol.* **153**, 8–18.
- Zhou, Z.Y., Thévenard, F., Barale, G. & Guignard, G. (2000) A new xeromorphic conifer from the Cretaceous of East China. *Palaeontology* **43**(3), 561–572.
- Zodrow, E.L., D'Angelo, J.A., Mastalerz, M., Cleal, C.J. & Keefe, D. (2010) Phytochemistry of the fossilized-cuticle frond *Macroneuropteris macrophylla* (Pennsylvanian seed fern, Canada). *Int. J. Coal Geol.* **84**, 71–82.